On the Mechanism of 5-Enolpyruvylshikimate-3-phosphate Synthase†

David L. Jakeman,‡ Dan J. Mitchell,‡ Wendy A. Shuttleworth,‡ and Jeremy N. S. Evans*

Department of Biochemistry and Biophysics, Washington State University, Pullman, Washington 99164-4660

Received June 4, 1998; Revised Manuscript Received July 13, 1998

ABSTRACT: 5-Enolpyruvylshikimate-3-phosphate (EPSP) synthase catalyzes the condensation of shikimate 3-phosphate (S3P) and phosphoenolpyruvate (PEP) to form EPSP, a precursor for the aromatic amino acids. This paper examines a recent claim [Studelska, D. R., McDowell, L. M., Espe, M. P., Klug, C. A., and Schaefer, J. (1997) *Biochemistry 36*, 15555−15560] that the mechanism of EPSP synthase involves two covalent enzyme−intermediates, in complete contrast to a large body of literature that has already proven the involvement of a single noncovalent intermediate. The evidence in the paper of Studelska et al. is examined closely, and unequivocal proof is provided that those authors' NMR assignments to covalent structures are in error, and that in fact the species they observed were simply the product EPSP and a side-product EPSP ketal. Since those authors used rotational-echo double-resonance (REDOR) solid-state NMR to measure intermolecular and intramolecular distances in the proposed covalent intermediates, we have used REDOR to measure the same distances in enzyme-free and enzyme-bound preparations of purified EPSP, and enzyme-free preparations of purified EPSP ketal. The distance between the shikimate ring phosphorus atom and C8 in enzyme-free EPSP is 6.6 ± 0.1 Å, which lengthens to 7.4 ± 0.1 Å in the presence of the enzyme, and in enzyme-free EPSP ketal is 5.6 ± 0.1 Å. These are entirely consistent with those measured by Studelska et al., which were 7.5 ± 0.5 Å for a putative enzyme−enolpyruvyl species and 6.1 ± 0.3 Å for a putative enzyme−ketal species.

A recent report appeared describing a "new and potentially general method of determining the pathway of an enzymatic reaction via solid-state magic-angle spinning (MAS)[1] NMR" (*1*). It was suggested that sub-zero temperature entrapment of intermediates of the enzyme 5-enolpyruvylshikimate-3-phosphate (EPSP) synthase had been achieved, and a new mechanism for the enzyme was proposed. In this paper, we provide conclusive proof that no catalytically competent enzyme−intermediates were detected by Studelska et al. and that their proposed mechanism is incorrect. Also the new method proposed by Studelska et al. does not yet afford a means for determining the pathway of an enzymatic reaction because their proposed 'intermediates' have not been demonstrated to turn over to products.

5-Enolpyruvylshikimate-3-phosphate (EPSP) synthase (EC 2.5.1.19) catalyzes the penultimate step in the aromatic amino acid biosynthetic pathway in higher plants and bacteria. EPSP (**4**) is formed from shikimate 3-phosphate (S3P, **1**) and phosphoenolpyruvate (PEP, **2**) (see Scheme 1A). The enzyme is a monomer (with no metal or cofactor requirements) with molecular weight $M_r = 46\,000$, and the cloned *E. coli* gene has been used to generate a hyperexpressing strain (*2*), so that the bacterial enzyme is available in gram quantities. Furthermore, EPSP synthase is the primary site of action of the herbicide glyphosate (*3*), or *N*-phosphonomethylglycine. This is a broad-spectrum post-emergence herbicide with worldwide applications in agriculture and horticulture, and is the active ingredient of Roundup. The molecular details for how glyphosate inhibits EPSP synthase still remain unclear (*4*).

This enzyme has been extensively studied by kinetic and biophysical methods in the last 10 years. The direct observation of the enzyme-bound intermediate (E·I, **3**) complex was first reported by our laboratory (*5*, *6*), and later confirmed by another laboratory (*7*). We have since characterized some site-directed mutants of the enzyme by steady-state kinetics, kinetic isotope effect analysis, fluorescence spectroscopy, and solution-state ^{31}P, ^{13}C, and ^{15}N NMR spectroscopy (*8*−*10*). We have also characterized the enzyme qualitatively by solid-state REDOR NMR spectroscopy (*vide infra*) (*11*), and recently completed a quantitative REDOR study (*12*). There are only and handful of enzymes for which the full kinetic and thermodynamic profile has been determined, and EPSP synthase is one of this select group largely as a result of work by Anderson and Johnson (*13*). One prediction from this work is that the E·I complex of this enzyme is unusually stable, and the enzyme destabilizes the intermediate and selectively interacts more tightly with the substrates and products. Although Anderson and Johnson postulated an equilibrium sequential ordered mechanism,

† This work was supported by NIH Grant GM43215. The WSU NMR Center equipment was supported by NIH Grants RR0631401 and RR12948 and by NSF Grants CHE-9115282 and DBI-9604689.

* Corresponding author: Department of Biochemistry and Biophysics, Washington State University, Pullman, WA 99164-4660. Telephone: (509)-335-6321. FAX: (509)-335-9688. EMAIL: evansj@wsu.edu.

‡ These authors contributed equally to this work.

[1] Abbreviations: CP-MAS, cross-polarization magic angle spinning; DTT, dithiothreitol; E·I, enzyme−intermediate; EPSP, 5-enolpyruvylshikimate 3-phosphate; EPSPS, 5-enolpyruvylshikimate-3-phosphate synthase; EPT, enolpyruvyltransferase; FID, free-induction decay; MAS, magic angle spinning; PEP, phosphoenolpyruvate; P_i, inorganic phosphate; REDOR, rotational-echo double-resonance; S3P, shikimate 3-phosphate; Δ*S*, REDOR difference; S_0, REDOR full echo; UDP-NAG, uridine diphosphate *N*-acetylglucosamine.

S0006-2960(98)01327-0 CCC: $15.00
Published on Web 08/12/1998

Scheme 1: (A) Current View of the Mechanism of EPSP Synthase. (B) Mechanism for EPSP Synthase Proposed by Studelska et al. (*1*).

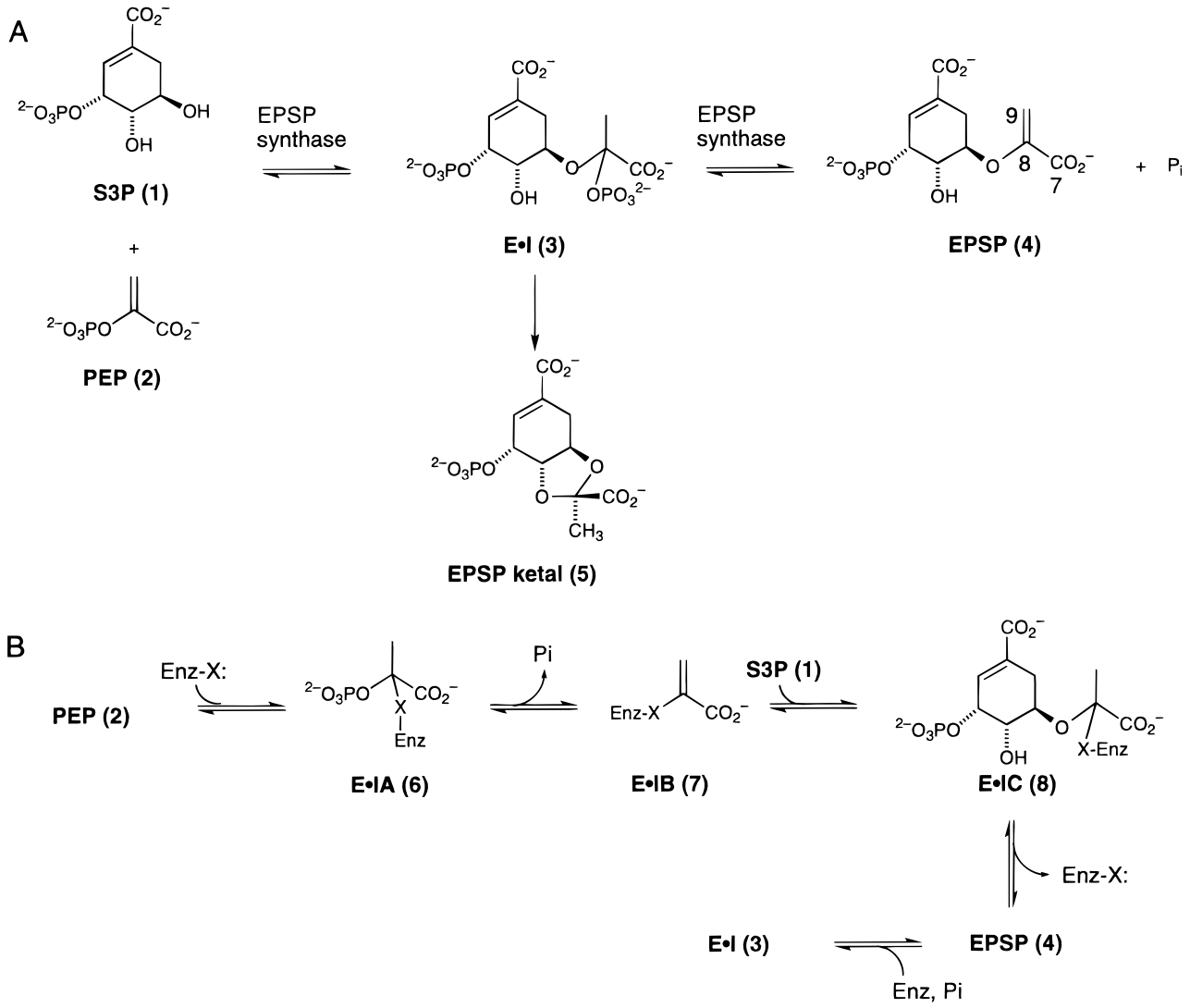

subsequent evidence suggests that a random kinetic mechanism is operating (*14*) which was confirmed by the observation that PEP can bind to the enzyme in the absence of S3P (*15*), and that EPSP and P_i can bind randomly (*16*). Another interesting result is the observation (*17*) that *Z*-fluoro-PEP acts as an inhibitor of EPSP synthase, competitive with respect to both S3P and PEP when the fixed substrate concentration was saturating, and mixed inhibition when the fixed substrate was nonsaturating. Furthermore, it appears that (*Z*)-fluoro-PEP is converted to the fluoro derivative of the tetrahedral intermediate (*17*), which remains tightly bound to the enzyme active site.

Despite the considerable body of evidence in favor of a noncovalent tetrahedral intermediate in the reaction catalyzed by EPSP synthase, Studelska et al. propose an alternate mechanism illustrated in Scheme 1B. In support of this mechanism, Studelska et al. cite the work of Anton et al. (*18*), who observed tritium incorporation at C3 of PEP in the presence of 4,5-dideoxy-S3P (not 5-deoxy-S3P as Studelska et al. suggest). What Studelska et al. fail to mention was that in the work of Anton et al., the incorporation of tritium was at a rate far below the turnover rate of the enzyme, implying a nonenzymatic or catalytically irrelevant process. Similarly, it was shown (*19*) that when EPSP synthase was incubated with 5-deoxy-S3P, slow exchange of deuterium into PEP occurred. Furthermore, our laboratory showed in 1989 that there was no evidence for the formation of a covalent intermediate in the presence of 4,5-dideoxy-S3P and PEP (*5*).

In this paper, we will examine the evidence presented by Studelska et al. in support of the mechanism shown in Scheme 1B, and provide conclusive proof that it is incorrect.

MATERIALS AND METHODS

Chemicals and Enzymes. All chemicals were purchased from Sigma (St. Louis, MO) except [2-^{13}C]PEP which was obtained from Cambridge Isotope Labs (Andover, MA), and [2,3-$^{13}C_2$]PEP which was obtained from MSD Isotopes (Canada). Shikimate 3-phosphate was isolated from cultures of *Klebsiella pneumoniae* (*20*) and purified as described previously (*2*). All enzyme manipulations were carried out at 4 °C unless indicated otherwise. EPSP synthase was dialyzed into potassium phosphate (20 mM, pH 7.0) prior to solution-state NMR.

Purification of Wild-Type EPSP Synthase. Wild-type EPSP synthase was overexpressed from *E. coli* BLR (λDE3)-

(pLysS)(pWS230) and purified by literature methods (*2*). The enzymes were stored at −78 °C in a buffer of Tris-HCl (50 mM, pH 7.8) and DTT (10 mM).

Enzyme Activity Assay and Protein Determination. EPSP synthase activity was routinely assayed by the reverse coupled assay of (*21*). Protein was determined by the method of (*22*) using bovine serum albumin as a protein standard.

Preparation of EPSP and EPSP Ketal. S3P (20 mg), PEP (20 mg), and EPSP synthase (5 mg) were reacted overnight in Tris-HCl (600 μL, 50 mM, pH 7.5) at 293 K. Ethanol (1.4 mL) was added and the sample centrifuged (8000*g*, 20 min, 277 K). The pellet was resuspended in EtOH (1 mL, 70%) and centrifuged again. The supernatants were combined and freeze-dried, and the resultant solid was redissolved and applied to an ion-exchange MonoQ FPLC column (Pharmacia-Biotech). EPSP eluted at 500 mM ammonium bicarbonate in a linear gradient (0−1 M, pH 9.0). [8-^{13}C]-EPSP was synthesized in a similar manner using [2-^{13}C]PEP. [8-^{13}C]EPSP ketal was prepared using phosphate buffer (20 mM) according to (*23*) and isolated by an ion-exchange MonoQ FPLC column. EPSP ketal eluted at 400 mM ammonium bicarbonate in a linear gradient (0−1 M, pH 9.0). NMR data (^{1}H, ^{13}C, and ^{31}P) and mass spectra for both molecules were consistent with the literature (*20*, *23*).

Solution-State NMR Spectroscopy. Solution ^{13}C NMR data were obtained on a Varian Inova 500 spectrometer operating at a ^{13}C frequency of 125.697 MHz and a ^{31}P frequency of 202.345 MHz. ^{13}C spectra were referenced to external dioxane in D_2O buffer (δ_C 67.4 ppm). The ^{31}P spectra were referenced to external H_3PO_4 (85%) (δ_P 0.00 ppm). All recycle times were 1 s. Sample temperature was maintained using an FTS Systems cooling unit and the Varian (Highland Inc.) variable temperature controller. Data were processed off-line on a Silicon Graphics O2 computer using FELIX97 (MSI).

Solid-State NMR Sample Preparation. All samples were shell-frozen in liquid N_2 prior to lyophilization for 16 h at a pressure of 70 mTorr. Sample 1 (enzyme-free [8-^{13}C]EPSP): [8-^{13}C]EPSP (5 mg) was dissolved in water (1 mL) with trehalose (95 mg). Sample 2 (enzyme-free EPSP) was prepared in an identical manner to sample 1. Sample 3 (EPSP synthase/[8-^{13}C]EPSP, 1:1 complex): [8-^{13}C]EPSP (156 μL, 14.1 mM) was added to EPSP synthase (2.21 mL, 46 mg mL^{-1}) and incubated for 1 h at 293 K before the addition of trehalose (102 mg). Sample 4 (EPSP synthase/EPSP, 1:1 complex): EPSP (177 μL, 5.7 mM) was added to EPSP synthase (707 μL, 65 mg mL^{-1}) and incubated for 1 h at 293 K before the addition of trehalose (46 mg). Sample 5 ([8-^{13}C]EPSP ketal): [8-^{13}C]EPSP ketal (1 mg) was dissolved in water (1 mL) with trehalose (99 mg).

Solid-State NMR Spectroscopy. All solid-state spectra were obtained on a Chemagnetics CMX-400 solid-state NMR spectrometer using a Pencil triple resonance probe and a 5 mm zirconia rotor, with 4 ± 0.01 kHz spinning speed and a temperature of 293 K (unregulated). The ^{1}H frequency was 400.083 MHz, the ^{31}P frequency was 161.957 MHz, and the ^{13}C frequency was 100.616 MHz for EPSP and 100.612 MHz for EPSP ketal. The ^{1}H $\pi/2$ pulse was 3.1 μs, the contact time was 1.5 ms, and the recycle time was 2 s. ^{13}C CP-MAS spectra was referenced to adamantane (δ_C 38.4 ppm). ^{31}P solid-state CP-MAS REDOR spectra were obtained using a literature pulse sequence (*24*) with *XY*-8 phase cycling, and with π-pulses of 6.2 and 8.0 μs for ^{31}P-refocusing and ^{13}C-dephasing, respectively. ^{1}H decoupling field strengths were 93 kHz (mixing) and 85 kHz (acquisition). Spectra were referenced to external H_3PO_4 (85%) (δ_P 0.0 ppm), and data were processed on a Sun Microsystems computer using FELIX95 (MSI).

Distance Determinations. Substantial ^{31}P dephasing was observed due to natural-abundance ^{13}C as well as expected ^{31}P dephasing due to labeled ^{13}C atoms. The natural-abundance dephasing was accounted for using (*24*):

$$\lambda_D^2 = (15/16)(1 - [1 - (\Delta S/S_0)_{obsd}]/[1 - (\Delta S/S_0)_{nat\ abnd}]) \quad (1)$$

where $(\Delta S/S_0)_{obsd}$ represents dephasing by label and background (samples 1, 3, and 5) and $(\Delta S/S_0)_{nat\ abnd}$ represents dephasing by background only (samples 2 and 4). This equation neglects ^{13}C−^{13}C dipolar coupling, and assumes that dephasing by the ^{13}C labels and the ^{13}C background are essentially independent. Dipolar coupling constants corrected for natural abundance were determined through the relationship $D = \lambda_D/N_cT_r$ and hence the corresponding distances calculated from $D = \gamma_P\gamma_C h/4\pi r^3$, where N_c is the number of rotor cycles of dephasing, T_r is the rotor period, r is the internuclear distance, and γ_P and γ_C are the phosphorus and carbon gyromagnetic ratios respectively. Data reported here were mostly in the reliable range for λ_D ($0.2 < \lambda_D < 0.5$), and generally did not display steady upward drifts of r with increasing N_c. Corrected $\Delta S/S_0$ values (data points in Figure 4) were then determined by exact simulation using the calculated dipolar coupling constants. The simulated REDOR dephasing curves (solid lines in Figure 4) were obtained from a dipolar coupling constant which was calculated from the average distance determined from distances corresponding to individual data for each rotor cycle in both molecules. Simulations were obtained by exact numerical evaluation (relaxation was not included) of the time-dependent propagator. The internal Hamiltonian explicit in the time-dependent propagator contained exact values for all isotropic interactions, as well as exact dipolar coupling values. Reasonable values were used for all chemical shift anisotropic interactions. With the use of the propagator and the density matrix, pertinent expectation values were obtained in the determination of S_1 and S_0 values. All code used was written in Fortran and run on a 16-processor IBM SP2 computer. The REDOR distances quoted are the mean of the distances calculated at each individual rotor cycle ± the standard deviation.

Molecular Dynamics Simulations. EPSP and EPSP ketal were modeled in Insight II (97.0) (MSI) using Discover to run the minimization and dynamics. Energy and charges were assigned using the CVFF forcefield; each structure was minimized (steepest gradient algorithm) prior to the dynamics run for 1000 iterations. During the dynamics run, the molecules were heated to 1000 K, equilibrated for 1000 steps, and then run for 10 000 steps over an 11 ps period. The dielectric constant was set to 78. All calculations were performed and displayed on a Silicon Graphics O2 computer.

RESULTS

Solution-State NMR Spectroscopy. Figure 1A shows the ^{1}H-decoupled ^{13}C NMR spectrum of EPSP synthase in the

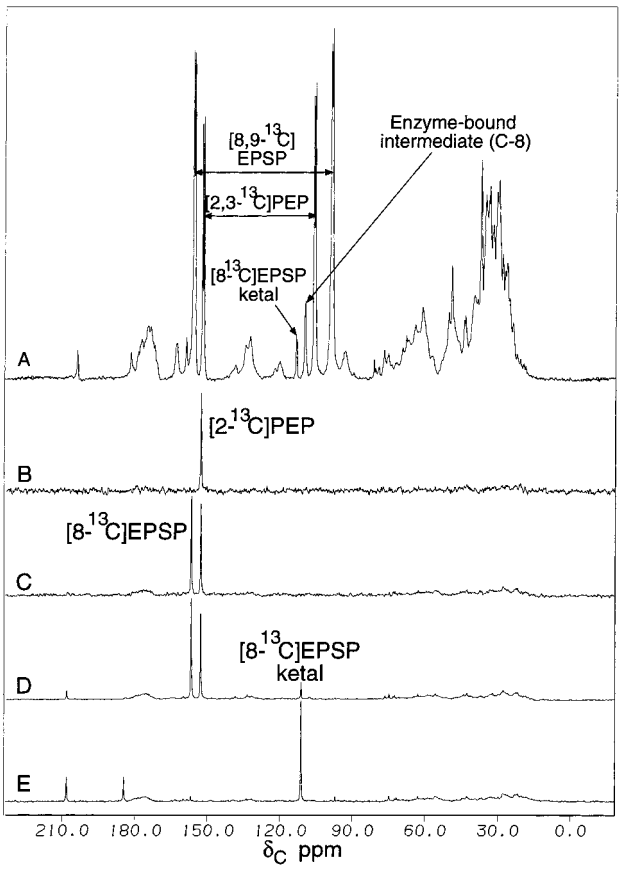

FIGURE 1: ^{1}H-decoupled ^{13}C solution-state NMR spectra of EPSP synthase plus substrates under equilibrium conditions and after long time periods. (A) Wild-type EPSP synthase (2.0 mM), potassium phosphate (20 mM, pH 7.0), D_2O (10%) plus S3P (10 mM) and [2,3-$^{13}C_2$]PEP (10 mM); (B) EPSP synthase (0.8 mM), potassium phosphate (20 mM, pH 7.2), D_2O (10%) plus [2-^{13}C]PEP (8 mM) (64 scans); (C) same as (B) plus S3P (8.0 mM) after 1 h (804 scans); (D) same as (C) after 15 h (2512 scans); (E) same as (D) after 48 h (3788 scans). Figure 1A was obtained at 277 K with 40 000 scans, a 4 μs pulse width, and a sweep width of 30 kHz, and FIDs were Fourier-transformed after zero-filling to 79K points with 20 Hz line broadening. Figure 1B−E was obtained at 293 K with a 3 μs pulse width and a sweep width of 35 kHz. FIDs were Fourier-transformed after zero-filling to 91K points with 20 Hz line broadening.

presence of S3P, [2,3-$^{13}C_2$]PEP, and inorganic phosphate under equilibrium conditions (*5*). As has been reported previously (*5*, *9*, *25*), resonances are evident due to the substrate PEP at 103.2 ppm (C2) and 152.4 ppm (C3), and the product EPSP at 95.7 ppm (C9) and 156.4 ppm (C8), in addition to resonances due to enzyme-bound EPSP at 88.9 ppm (C9) and 164.8 ppm (C8), enzyme-bound tetrahedral intermediate (107.2 ppm, C8), and enzyme-free EPSP ketal (110.9 ppm, C8). The EPSP ketal was first reported by our laboratory (*5*), although at the time incorrectly identified as an enzyme-free intermediate. Work by Anderson, Johnson, and co-workers (*7*, *23*) showed the species to be the EPSP ketal, with a rate of formation on the order of 4×10^{-5} s^{-1}, which when added back to the enzyme is not converted to substrate or product, all suggesting that it is a side-product formed irreversibly off the main enzymatic pathway. This is illustrated in Figure 1B−E, in which EPSP synthase is incubated with S3P and [2-^{13}C]PEP under equilibrium conditions where the tetrahedral enzyme−intermediate accumulates. Over extended periods of time, the EPSP ketal peak grows at the expense of initially the PEP resonance

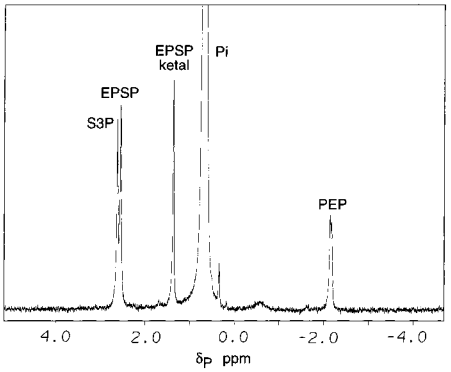

FIGURE 2: ^{1}H-decoupled solution-state ^{31}P NMR spectrum of EPSP synthase (0.8 mM) plus S3P (8.0 mM) and [2-^{13}C]PEP (8.0 mM) at 293 K acquired after Figure 1 spectrum C. 2608 scans were obtained with a 1 s recycle time, a 3 μs pulse width, and a sweep width of 10 kHz. FIDs were Fourier-transformed after zero-filling to 32K points with 20 Hz line broadening.

and then eventually the EPSP resonance. In addition to the ketal, other byproducts form including pyruvate and pyruvate dimer (4-hydroxy-4-methylketoglutarate), which have been reported previously (*5*).

Figure 2 shows the ^{1}H-decoupled ^{31}P NMR spectrum of the same sample as in Figure 1D, showing the ^{31}P resonances for S3P (2.62 ppm), PEP (−2.16 ppm), EPSP (2.55 ppm), inorganic phosphate (0.68 ppm), and EPSP ketal (1.38 ppm). These results are consistent with those reported by Leo et al. (*23*).

Solid-State NMR Spectroscopy. Figure 3A,B shows the ^{1}H-decoupled ^{13}C CP-MAS solid-state NMR spectra of purified [8-^{13}C]EPSP (Figure 3A) and [8-^{13}C]EPSP ketal (Figure 3B). In addition to resonances from trehalose and its associated rotational side-bands, the isotropic resonance of [8-^{13}C]EPSP occurs at 154.4 ppm, and of [8-^{13}C]EPSP ketal at 108.5 ppm. Resonances due to enzyme-bound EPSP and enzyme-free EPSP cannot easily be distinguished on the basis of chemical shift in the solid state. REDOR NMR was carried out with ^{13}C dephasing pulses placed with their carrier position at either 154 ppm for EPSP or 108 ppm for EPSP ketal, and a representative ^{31}P full echo spectrum of [8-^{13}C]-EPSP with trehalose is shown in Figure 3C and a REDOR difference spectrum obtained with ^{13}C dephasing at C8 shown in Figure 3D. Similarly, a ^{31}P full echo spectrum of enzyme-bound [8-^{13}C]EPSP with trehalose is shown in Figure 3E and a REDOR difference spectrum obtained with ^{13}C dephasing at C8 shown in Figure 3F. Note that the enzyme-bound resonance is narrower than enzyme-free EPSP, presumably because of differences in sample heterogeneity. This narrower resonance for the enzyme-bound species was used in the subsequent REDOR calculations. REDOR data were collected for three different samples: [8-^{13}C]EPSP lyophilized from a trehalose solution; [8-^{13}C]EPSP plus EPSP synthase lyophilized from a trehalose solution; and [8-^{13}C]-EPSP ketal lyophilized from a trehalose solution, and the data are shown in Figure 4. The samples were all lyophilized from trehalose because of the advantageous effects it has on solid-state NMR line widths (*26*). Equivalent data were also collected on samples of unlabeled EPSP with trehalose, and for unlabeled enzyme-bound EPSP plus trehalose, in order to obtain corrections due to dephasing from natural-abundance ^{13}C in the samples. The data from the unlabeled EPSP with trehalose were used to correct the data from

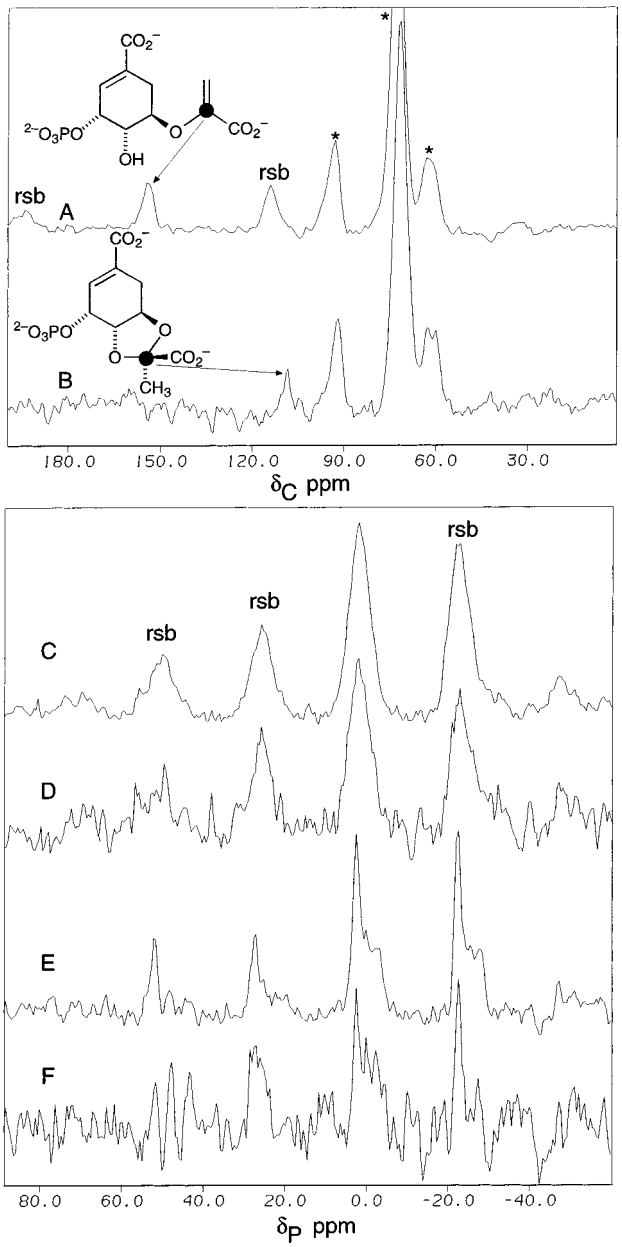

FIGURE 3: ^{1}H-decoupled solid-state CP-MAS (A) ^{13}C NMR spectra of enzyme-free EPSP (sample 1, 209 scans, sweep width 50 kHz) with C8 at 155 ppm; (B) ^{13}C NMR spectra of enzyme-free EPSP ketal with C8 at 111 ppm (sample 5, 297 scans, sweep width 30 kHz); (C) ^{31}P-detected, ^{13}C-dephased REDOR NMR spectra of EPSP plus trehalose (sample 1), S_0 spectrum, and (D) ΔS spectrum. (e) ^{31}P-detected, ^{13}C-dephased REDOR NMR spectra of enzyme-bound EPSP (sample 4), S_0 spectrum, and (F) ΔS spectrum. Rotational side-bands are indicated with a 'rsb', and trehalose signals with an asterisk. REDOR spectra (C−F) were obtained at 48 rotor cycles with 4096 scans (C, D) and 204 800 scans (E, F) and a sweep width of 40 kHz. FIDs were Fourier-transformed after zero-filling to 512 points with 100 Hz line broadening.

[8-^{13}C]EPSP ketal with trehalose. The natural-abundance corrections were carried out as detailed under Materials and Methods, using eq 1. When $(\Delta S/S_0)_{\text{nat abund}}$ values are subtracted from $(\Delta S/S_0)_{\text{obsd}}$ values and the resultant corrected $(\Delta S/S_0)$ values fitted to a universal curve, the distances calculated by this method are 0.1−0.3 Å longer than those obtained by eq 1, as observed by McDowell et al. (*27*).

Molecular Dynamics Calculations. Figure 5 shows the results of a molecular dynamics simulation for EPSP and

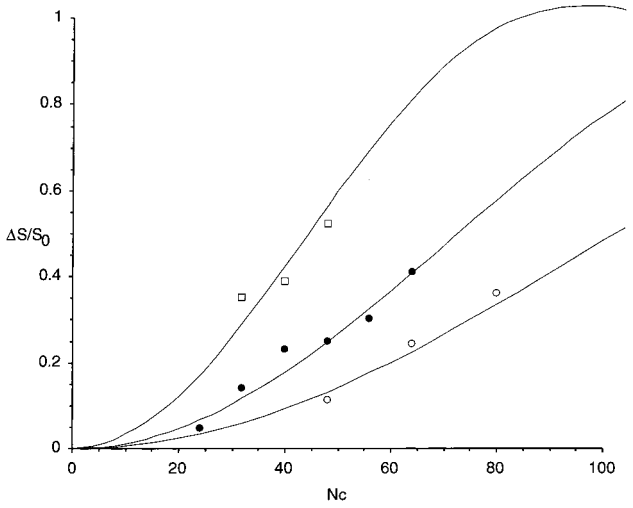

FIGURE 4: ^{31}P REDOR $(\Delta S/S_0)$ data with dephasing on ^{13}C, corrected for natural-abundance ^{13}C (*24*). (□) Enzyme-free EPSP ketal (sample 5 corrected for natural abundance using sample 2); (●) enzyme-free EPSP (sample 1 corrected for natural abundance using sample 2); and (○) EPSP/EPSP synthase (1:1) complex (sample 3 corrected for natural abundance using sample 4). The solid lines represent simulated dephasing curves for the average distance determined for each molecule.

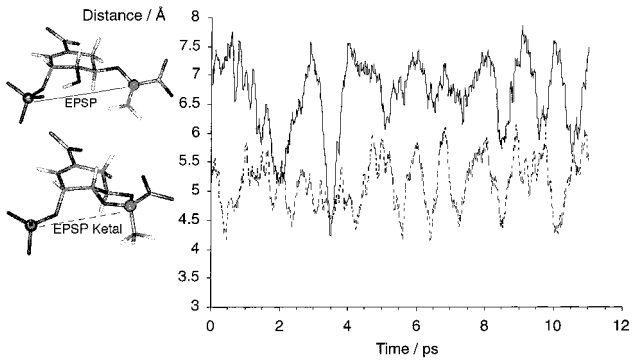

FIGURE 5: Molecular dynamics simulation on EPSP and EPSP ketal. The solid line represents the distance between the phosphorus atom and C8 of EPSP (average 6.7 Å). The dashed line represents the distance between the phosphorus atom and C8 of EPSP ketal (average 5.1 Å). Molecular models for EPSP and EPSP ketal are shown adjacent to their relevant plots, with the phosphorus atom and C8 of each molecule drawn as balls.

for EPSP ketal *in vacuo* with a dielectric constant approximating solvent water, showing the variation in distances between C8 and the ring phosphate phosphorus atom with time. The average distances obtained in the simulations were 5.1 Å for EPSP ketal and 6.7 Å for EPSP, with ranges of 4.2−6.2 Å and 4.2−7.9 Å, respectively.

DISCUSSION

The work of Studelska et al. (*1*) provided solid-state NMR evidence for two purportedly novel species occurring with time under conditions in which two different multiple mutants (N94S, I113M, F172W, W289Q; and F172W, W289Q) were lyophilized in the presence of substrates, or wild-type enzyme was cooled to −30 °C before addition of S3P and [2-^{13}C]PEP and subsequent lyophilization. These two species appeared at ^{13}C solid-state NMR chemical shifts of 155 ppm and at 108 ppm. These were interpreted as arising from putative intermediate **7** (see Scheme 1B) for the species at 155 ppm and from putative intermediate **8** for

the species at 108 ppm. Evidence was presented that showed that the species at 155 ppm disappeared with time, with concomitant appearance of the species at 108 ppm. However, no evidence was presented that the species at 108 ppm could be converted to the product, EPSP. $^{31}P-^{13}C$ REDOR measurements provided evidence that the distance between the labeled ^{13}C and a nearby phosphorus atom with the wild-type enzyme was 7.5 ± 0.5 Å for the species at 155 ppm (putatively species **7**) and 6.1 ± 0.3 Å for the species at 108 ppm (putatively species **8**). This was interpreted as providing evidence for an intermolecular distance being measured between a phosphorus and species **7** for the 155 ppm species, and an intramolecular distance between a phosphorus atom and C8 of species **8** for the 108 ppm species, as a result of some condensation event. We argue, on the basis of the vast body of literature already presented (*vide supra et infra*) along with our new results presented here, that Studelska et al. (*1*) are in error in their solid-state NMR spectral assignments, and that the species observed at 155 ppm is simply EPSP (**4**), and the species at 108 ppm is simply the EPSP ketal (**5**).

The results in Figure 1A show clearly that under equilibrium conditions both EPSP and EPSP ketal can be present at the same time as the noncovalent tetrahedral intermediate. Furthermore, Figure 1B−E establishes that the EPSP ketal forms ultimately at the expense of both PEP and EPSP. A likely explanation for this is that the EPSP ketal forms from an intramolecular S_N2 reaction of the shikimate ring 4-hydroxyl with the tetrahedral carbon of the noncovalent intermediate, although the mechanistic details of this process are at present unclear. Since the enzyme is freely reversible, as the intermediate slowly turns over to form the EPSP ketal side-product, the PEP and EPSP pools are depleted through conversion into intermediate. There are also additional drains on the PEP pool from conversion of PEP to pyruvate and pyruvate dimer after long periods of time. The evidence in support of the formation of the EPSP ketal from the tetrahedral intermediate comes from the observation that it can form in either the forward or the reverse reaction at the expense of the tetrahedral intermediate, and when added back to the enzyme, does not result in substrate or product formation (*7*, *23*).

The results in Figure 2 show the pertinent ^{31}P solution-state chemical shifts for EPSP and EPSP ketal. The ^{31}P chemical shifts were not reported by Studelska et al. (*1*) for the two putative intermediates they propose; however, it is quite likely that they will roughly correspond (within the error of differences in referencing) to those we report here for EPSP and EPSP ketal. Figure 3A,B shows the solid-state ^{13}C chemical shifts for purified EPSP and EPSP ketal, and their shifts at 154 and 108 ppm, respectively, correspond very closely with the 155 and 108 ppm species reported by Studelska et al. (*1*). The REDOR results shown in Figures 3C−F and 4 provide clear evidence that the intramolecular distance between the shikimate ring phosphorus atom and C8 in enzyme-free EPSP is 6.6 ± 0.1 Å, which lengthens to 7.4 ± 0.1 Å in the presence of the enzyme (Figure 3E,F), and in enzyme-free EPSP ketal is 5.6 ± 0.1 Å. A search of conformational space available to these atoms was performed by molecular dynamics simulation, as shown in Figure 5, and average distances for free EPSP were found to be 6.7 Å, although the range went up to 7.9 Å, and for EPSP ketal was 5.1 Å. This suggests that the enzyme-bound form of EPSP adopts a more extended conformation than when not bound to the enzyme. In addition, these distances obtained for EPSP and EPSP ketal are consistent within error of the values reported by Studelska et al. (*1*) and given above.

The work by Studelska et al. (*1*) failed to provide any proof of the existence of a covalent enzyme−intermediate. Although the mechanism shown in Scheme 1B postulates the involvement of an enzyme nucleophile, no evidence was presented by Studelska et al. (*1*) that a candidate residue had been identified. Many of the residues in the enzyme active site have already been identified (*8*−*10*, *28*−*34*), and those that are potential nucleophiles have been ruled out as being catalytically irrelevant. Indeed, Studelska et al. (*1*) fail to provide any proof that the species they detected are in any way covalently attached to EPSP synthase. Furthermore, Studelska et al. (*1*) cite the work of Walsh and co-workers (*35*) on the detection of a covalent *O*-phosphothioketal enzyme intermediate of the related enzyme uridine diphosphate-*N*-acetylglucosamine (UDP-NAG) enolpyruvyltransferase (EPT), one of a class of at least four enolpyruvyl transfer enzymes. However, Studelska et al. (*1*) fail to point out that Anderson, Walsh, and co-workers first reported the detection of a noncovalent tetrahedral intermediate (*36*). In fact, it was work from Amrhein's group (*37*) that first showed that a stable and isolatable covalent species forms, in which PEP is attached to the enzyme through cysteine-115 in a *O*-phosphothioketal. This was also detected by NMR in our laboratory (*38*) and independently by Anderson, Walsh, and co-workers (*35*). They also carried out preliminary pre-steady-state kinetics, which appear to suggest that the covalent species is turned over at rates consistent with being on the reaction pathway. Further evidence in support of a covalent intermediate was provided by Walsh and co-workers (*39*, *40*). However, more recently Walsh and co-workers (*41*, *42*) have concluded that the covalent intermediate is on a branched pathway in the enzymatic mechanism, rather than on the primary pathway, in which the enzyme nucleophile can intercept the oxocarbenium ion derived from PEP in competition with interception by the cosubstrate nucleophile. Fairly compelling evidence for this has come from analysis of the role of Cys-115 by examination of a C115D mutant (*43*) which retained activity, implying that the primary role of Cys-115 is as a general acid, and that the formation of the covalent adduct is through the secondary role of Cys-115 as a nucleophile. The X-ray crystal structure of a stable noncovalent enzyme−intermediate complex derived from (*Z*)-3-fluoro-PEP has also been reported (*44*). While the precise mechanistic details of the EPT enzyme remain to be fully elucidated, the parallel with EPSP synthase drawn by Studelska et al. (*1*) is not consistent with the most recent data.

Studelska et al. (*1*) also failed to provide any proof of the existence of a true enzyme−intermediate, covalent or otherwise. The need to demonstrate kinetic competence has already been widely documented in the literature (*45*−*47*). Our own laboratory failed to do this when we first reported the species later identified to be the EPSP ketal (*5*). Studelska et al. (*1*) failed to demonstrate that the species they detected turned over at a rate consistent with the rate of the enzymatic reaction. Furthermore, they did not provide convincing evidence that they were even able to detect the known

noncovalent tetrahedral intermediate (**3**). A ^{31}P-detected ^{13}C-dephased REDOR spectrum was presented that showed strong dephasing, which they interpreted as arising from intermediate **3**, but in the absence of ^{31}P NMR assignments, this provides no evidence for their detection of intermediate **3**. In contrast, our laboratory has previously used both solution-state NMR and time-resolved solid-state NMR to detect and characterize intermediate **3**. Our time-resolved solid-state NMR work showed for the first time that it was possible to use solid-state NMR to follow the buildup of the intermediate (with concomitant loss of substrate and buildup of product) under pre-steady-state kinetic conditions. These studies established clearly that the intermediate formed from the substrates or products, with pre-steady-state kinetics consistent with those reported by Anderson and Johnson (*13*) determined by chemical quench methods. The time-resolved solid-state NMR experiments were performed in rapidly frozen solution maintained at low temperature (<-50 °C). We have even used ^{31}P-dephased ^{13}C-detected REDOR to detect intermediate **3** using an approach we call time-resolved solid-state REDOR-edited NMR detection (*48*). Also, Anderson and co-workers have reported the detection of intermediate **3** by electrospray mass spectrometry (*49*) under pre-steady-state conditions. Thus, the work by Studelska et al. (*1*) suggests that they were following very slow steady-state kinetic processes involving the formation of product and a side-product in the solid state. They did not detect any enzyme−intermediates, or provide any evidence for the species they detected being covalently attached to the enzyme. More importantly, they failed to show turnover of their proposed 'intermediates' to products, and their claim of describing a new and potentially general method of determining the pathway of an enzymatic reaction via solid-state NMR has yet to be proved. Their work demonstrates the danger of overinterpreting NMR data on the basis of a limited set of chemical shifts and REDOR distances, particularly against a wealth of high-resolution NMR data and sophisticated kinetic and bioorganic studies.

ACKNOWLEDGMENT

We thank Greg Helms, WSU NMR Center Facility Manager, for his expert technical assistance.

REFERENCES

1. Studelska, D. R., McDowell, L. M., Espe, M. P., Klug, C. A., and Schaefer, J. (1997) *Biochemistry 36*, 15555−15560.
2. Shuttleworth, W. A., Hough, C. D., Bertrand, K. P., and Evans, J. N. S. (1992) *Protein Eng. 5*, 461−466.
3. Steinrucken, H. C., and Amrhein, N. (1984) *Eur. J. Biochem. 143*, 351−357.
4. Sikorski, J. A., and Gruys, K. J. (1997) *Acc. Chem. Res. 30*, 2−8.
5. Barlow, P. N., Appleyard, R. J., Wilson, B. J. O., and Evans, J. N. S. (1989) *Biochemistry 28*, 7985−7991 and correction p 10093.
6. Evans, J. N. S. (1992) *NMR and Enzymes* in *Pulsed Magnetic Resonance: NMR, ESR and Optics (A Recognition of E. L. Hahn)*, Oxford University Press, Oxford and New York.
7. Anderson, K. S., Sammons, R. D., Leo, G. C., Sikorski, J. A., Benesi, A. J., and Johnson, K. A. (1990) *Biochemistry 29*, 1460−1465.
8. Shuttleworth, W. A., and Evans, J. N. S. (1996) *Arch. Biochem. Biophys. 334*, 37−42.
9. Shuttleworth, W. A., and Evans, J. N. S. (1994) *Biochemistry 33*, 7062−7068.
10. Shuttleworth, W. A., and Evans, J. N. S. (1998) *Biochemistry* (submitted for publication).
11. Li, Y., Appleyard, R. J., Shuttleworth, W. A., and Evans, J. N. S. (1994) *J. Am. Chem. Soc. 116*, 10799−10800.
12. Jakeman, D. L., Mitchell, D. J., Shuttleworth, W. A., and Evans, J. N. S. (1998) *Biochemistry* (submitted for publication).
13. Anderson, K. S., Sikorski, J. A., and Johnson, K. A. (1988) *Biochemistry 27*, 7395−7406.
14. Gruys, K. J., Walker, M. C., and Sikorski, J. A. (1992) *Biochemistry 31*, 5534−5544.
15. Ream, J. E., Yuen, H. K., Frazier, R. B., and Sikorski, J. A. (1992) *Biochemistry 31*, 5528−5534.
16. Gruys, K. J., Marzabadi, M. R., Pansegrau, P. D., and Sikorski, J. A. (1993) *Arch. Biochem. Biophys. 304*, 345−351.
17. Walker, M. C., Jones, C. R., Somerville, R. L., and Sikorski, J. A. (1992) *J. Am. Chem. Soc. 114*, 7601−7603.
18. Anton, D. L., Hedstrom, L., Fish, S. M., and Abeles, R. H. (1983) *Biochemistry 22*, 5903−5908.
19. Pansegrau, P. D., Anderson, K. S., Widlanski, T., Ream, J. E., Sammons, R. D., Sikorski, J. A., and Knowles, J. R. (1991) *Tetrahedron Lett. 32*, 2589−2592.
20. Bondinell, W. E., Vnek, J., Knowles, P. F., Sprecher, M., and Sprinson, D. B. (1971) *J. Biol. Chem. 246*, 6191−6196.
21. Lewendon, A., and Coggins, J. R. (1983) *Biochem. J. 213*, 187−191.
22. Bradford, M. M. (1976) *Anal. Biochem. 72*, 248−254.
23. Leo, G. C., Sikorski, J. A., and Sammons, R. D. (1990) *J. Am. Chem. Soc. 112*, 1653−1654.
24. McDowell, L. M., Klug, C. A., Beusen, D. D., and Schaefer, J. (1996) *Biochemistry 35*, 5395−5403.
25. Evans, J. N. S. (1996) *Biomolecular NMR Spectroscopy*, Oxford University Press, Oxford and New York.
26. Jakeman, D. L., Mitchell, D. J., Shuttleworth, W. A., and Evans, J. N. S. (1998) *J. Biomol. NMR* (in press).
27. McDowell, L. M., Schmidt, A., Cohen, E. R., Studelska, D. R., and Schaefer, J. (1996) *J. Mol. Biol. 256*, 160−171.
28. Sost, D., and Amrhein, N. (1990) *Arch. Biochem. Biophys. 282*, 433−436.
29. Selvapandiyan, A., Ahmad, S., Majumder, K., Arora, N., and Bhatnagar, R. K. (1996) *Biochem. Mol. Biol. Int. 40*, 603−610.
30. Selvapandiyan, A., Majumder, K., Fattah, F. A., Ahmad, S., Arora, N., and Bhatnagar, R. K. (1995) *FEBS Lett. 374*, 253−256.
31. Padgette, S. R., Huynh, Q. K., Aykent, S., Sammons, R. D., Sikorski, J. A., and Kishore, G. M. (1988) *J. Biol. Chem. 263*, 1798−1802.
32. Huynh, Q. K. (1991) *Arch. Biochem. Biophys. 284*, 407−412.
33. Huynh, Q. K., Kishore, G. M., and Bild, G. S. (1988) *J. Biol. Chem. 263*, 735−739.
34. Huynh, Q. K. (1988) *J. Biol. Chem. 263*, 11631−11635.
35. Brown, E. D., Marquardt, J. L., Lee, J. P., Walsh, C. T., and Anderson, K. S. (1994) *Biochemistry 33*, 10638−10645.
36. Marquardt, J. L., Brown, E. D., Walsh, C. T., and Anderson, K. S. (1993) *J. Am. Chem. Soc. 115*, 10398−10399.
37. Wanke, C., and Amrhein, N. (1993) *Eur. J. Biochem. 218*, 861−870.
38. Ramilo, C., Appleyard, R. J., Wanke, C., Krekel, F., Amrhein, N., and Evans, J. N. S. (1994) *Biochemistry 33*, 15071−15079.
39. Kim, D. H., Lees, W. J., and Walsh, C. T. (1994) *J. Am. Chem. Soc. 116*, 6478−6479.
40. Marquardt, J. L., Brown, E. D., Lane, W. S., Haley, T. M., Ichikawa, Y., Wong, C. H., and Walsh, C. T. (1994) *Biochemistry 33*, 10646−10651.
41. Kim, D. H., Lees, W. J., Haley, T. M., and Walsh, C. T. (1995) *J. Am. Chem. Soc. 117*, 1494−1502.
42. Lees, W. J., and Walsh, C. T. (1995) *J. Am. Chem. Soc. 117*, 7329−7337.
43. Kim, D. H., Lees, W. J., Kempsell, K. E., Lane, W. S., Duncan, K., and Walsh, C. T. (1996) *Biochemistry 35*, 4923−4928.

44. Skarzynski, T., Kim, D. H., Lees, W. J., Walsh, C. T., and Duncan, K. (1998) *Biochemistry 37*, 2572−2577.
45. Cleland, W. W. (1990) *Biochemistry 29*, 3194−3197.
46. Anderson, K. S., and Johnson, K. A. (1990) *J. Biol. Chem. 265*, 5567−5572.
47. Anderson, K. S., and Johnson, K. A. (1990) *Chem. Rev. 90*, 1131−1149.
48. Mitchell, D. J., Jakeman, D. L., Igumenova, T. I., Shuttleworth, W. A., Miller, K. D., and Evans, J. N. S. (1997) *Chem. Comm.*, 1019−1020.
49. Paiva, A. A., Tilton, R. F., Jr., Crooks, G. P., Huang, L. Q., and Anderson, K. S. (1997) *Biochemistry 36*, 15472−15476.

BI9813274